AFRL-RY-WP-TR-2021-0050

RF PHOTONIC APPLICATIONS (Preprint)

Preetpaul Devgan

Highly Integrated Microsystems Branch
Aerospace Components & Subsystems Division

MARCH 2021
Final Report

AIR FORCE RESEARCH LABORATORY
SENSORS DIRECTORATE
WRIGHT-PATTERSON AIR FORCE BASE, OH 45433-7320
AIR FORCE MATERIEL COMMAND
UNITED STATES AIR FORCE

REPORT DOCUMENTATION PAGE

Form Approved
OMB No. 0704-0188

1. REPORT DATE *(DD-MM-YY)*	2. REPORT TYPE	3. DATES COVERED *(From - To)*
March 2021	Book Chapter Preprint	26 February 2021 –26 February 2021

4. TITLE AND SUBTITLE
RF PHOTONIC APPLICATIONS (Preprint)

5a. CONTRACT NUMBER
N/A

5b. GRANT NUMBER

5c. PROGRAM ELEMENT NUMBER
N/A

6. AUTHOR(S)
Preetpaul Devgan

5d. PROJECT NUMBER
N/A

5e. TASK NUMBER
N/A

5f. WORK UNIT NUMBER
N/A

7. PERFORMING ORGANIZATION NAME(S) AND ADDRESS(ES)

Air Force Research Laboratory
Sensors Directorate
Wright-Patterson Air Force Base, OH 45433-7320
Air Force Materiel Command
United States Air Force

8. PERFORMING ORGANIZATION REPORT NUMBER

9. SPONSORING/MONITORING AGENCY NAME(S) AND ADDRESS(ES)

Air Force Research Laboratory
Sensors Directorate
Wright-Patterson Air Force Base, OH 45433-7320
Air Force Materiel Command
United States Air Force

10. SPONSORING/MONITORING AGENCY ACRONYM(S)
AFRL/RYDI

11. SPONSORING/MONITORING AGENCY REPORT NUMBER(S)
AFRL-RY-WP-TR-2021-0050

12. DISTRIBUTION/AVAILABILITY STATEMENT
Approved for public release; distribution is unlimited.

13. SUPPLEMENTARY NOTES
PAO case number AFRL-2021-0601, Clearance Date 26 February 2021. Book chapter on RF Photonic Applications for the Encyclopedia of RF and Microwave Engineering. This is a work of the U.S. Government and is not subject to copyright protection in the United States. Report contains color.

14. ABSTRACT

Radio Frequency (RF) photonics seeks to address high speed analog signal processing applications that are not achievable by electronics. Applications where RF photonics provide advantages include the antenna remoting of analog signals, generation of low phase noise clock signals, isolation of RF signals and many others. Specifically, the need to access higher frequencies and wider bandwidths has driven the use of RF photonics for these applications. Because of the inherent wideband nature of photonics, it is an ideal solution to address these requirements.

15. SUBJECT TERMS
RF Photonics

16. SECURITY CLASSIFICATION OF:			17. LIMITATION OF ABSTRACT:	18. NUMBER OF PAGES	19a. NAME OF RESPONSIBLE PERSON (Monitor)
a. REPORT	b. ABSTRACT	c. THIS PAGE			Preetpaul Devgan
Unclassified	Unclassified	Unclassified	SAR	19	19b. TELEPHONE NUMBER *(Include Area Code)* N/A

Chapter RF Photonic Applications

1.0 Introduction

Radio Frequency (RF) photonics seeks to address high speed analog signal processing applications that are not achievable by electronics. Applications where RF photonics provide advantages include the antenna remoting of analog signals, generation of low phase noise clock signals, isolation of RF signals and many others. Specifically, the need to access higher frequencies and wider bandwidths has driven the use of RF photonics for these applications. Because of the inherent wideband nature of photonics, it is an ideal solution to address these requirements.

1.1 Need for RF Photonics

One prime example for the need to operate at higher frequencies is 5G communications. 5G is the latest standard for cellular communication networks [1]. The standard increases the bandwidth available to users, allowing for faster downloads and lag-free streaming of high definition videos. 5G achieves this enhanced capability by using frequency bands in the millimeter wave range (30-300 GHz). RF photonics can play a role in 5G by generating millimeter wave frequency carriers, as well as in the separation of transmitted and received signals at these frequency bands.

5G signals in the millimeter wave band also experience higher attenuation due to the materials used in buildings. The losses can limit the signal from reaching users in their apartments or offices. In order to overcome this obstacle, a Radio over Fiber link may be used to supply each apartment or office access to a wireless signal [2]. From the central station, a fiber optic cable can be run to each individual space in the building. The fiber optic cable will directly feed an antenna, creating a picocell. With millimeter wave frequencies, the signal from the access point will be attenuated enough as not to interfere with any neighboring signal.

Another application is radio astronomy. Large radio astronomy antenna arrays use multiple antennas, which are spaced over many kilometers from each other. By using an array, the increased gain allows for the detection of very faint radio waves from distant starts. In order to recover the detected signal, each antenna must be connected to a central base station. Due to the long lengths involved, a low-loss connection must be used. RF photonic links provide a link with low loss that can operate at frequencies in the millimeter wave band.

1.2 RF photonic advantages

One of the key advantages to using RF photonics is the fiber optic cable. The fiber optic line offers many advantages in comparison to electronic equivalents. RF photonic signals travel over a single mode fiber optic cable that contains a very small, cylindrical piece of glass. The electronic equivalent is a coaxial cable, which uses copper for the inner conductor. Fiber optic cables have been engineered to have losses that approach the Rayleigh scattering limit. The loss of an optical fiber as a function of wavelength appear in Figure 1. While the losses are dominated by water ion peaks around 1250 nm and 1400 nm, the minimum loss window is from 1510 nm to 1600 nm, where most fiber optic communication links operate. By selecting a laser source within this window, the loss as a function of distance will be 0.2 dB/km. Since the loss does not change over this 90 nm range, it is equivalent to having a cable whose RF loss is flat over approximately

11.25 THz. No coaxial or waveguide-based electronic cable exists that can compete with this loss over such a large bandwidth.

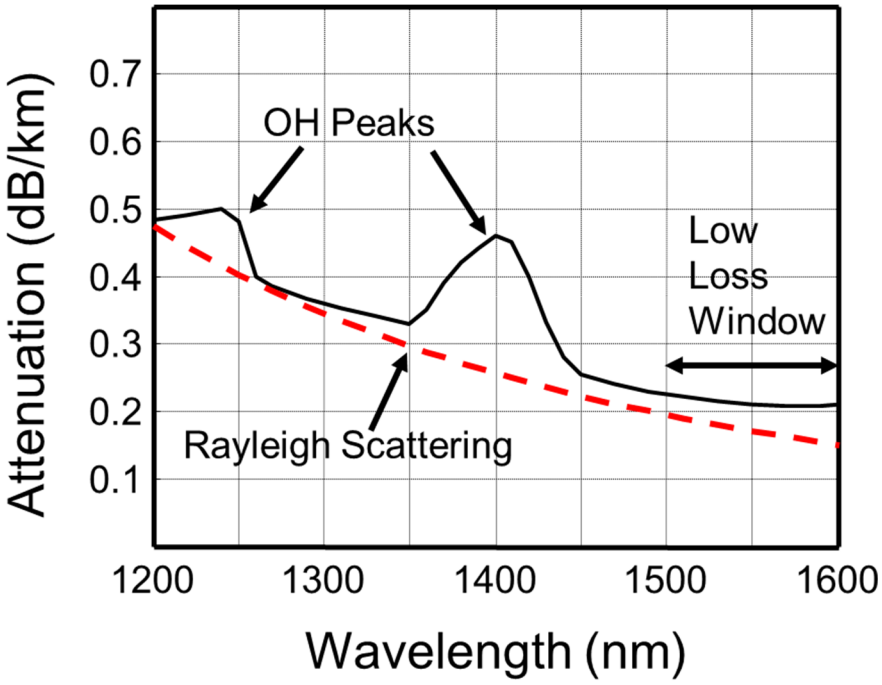

Figure 1. Loss of fiber optic cable in dB/km as a function of wavelength from 1200 to 1600 nm

When compared to coaxial cable, another set of advantages of fiber optic cables are size, weight and cost. The diameter of a fiber optic cable is on the order of 100's of microns, while a coaxial cable diameter is on the order of millimeters. The weight of a 30 m length of fiber optic cable is approximately hundreds of grams, while the same length of coaxial cable is on the order of ten kilograms. Finally, while copper is a valuable metal that is often scavenged for money, glass is cheap and not easily sold for scrap.

For many applications, phase stability between multiple links is essential. Most of the phase changes that occur are due to thermal effects, which changes the physical delay path of the link. Glass has a lower thermal coefficient of delay (TCD) when compared to copper, making fiber optic cables more phase stable than coaxial ones [3]. As glass is an electrical insulator, optical fibers are immune to electromagnetic interference. Additionally, a large electrical discharge, such as a lightning strike, will not propagate down a fiber optic cable, destroying any sensitive systems at the end of the link. Fiber optic cables do not build up static charges, allowing them to be used in flammable environments like a fuel tank. Finally, fiber optic cables can be easily hidden or buried without being found by metal detectors, unlike a coaxial cable.

1.3 Examples of RF Photonic Applications

Clearly, RF photonics offers advantages over other existing solutions for analog systems. The rest of this chapter will highlight some applications where photonics are used to best make use of these advantages. While many applications exist, three in particular will be explored. They are antenna remoting, oscillators and signal isolation. Each of these application spaces will be reviewed and examples of photonic based systems' performance will be provided.

2.0 Antenna remoting applications

One application using RF photonics is a link for antenna remoting. Antenna remoting involves transporting a spectrum of RF signals from an antenna site to a remote processor. An example of an RF photonic link appears in Figure 2. The link consists of an optical source (often a semiconductor-based laser), whose output is connected to an electro-optic modulator (EOM). The RF signals are up-converted onto the laser light via the EOM. The output of the EOM is then passed through an optical amplifier (OA) in order to compensate for the losses of the EOM and set the optical power to as high as possible. The amplified light is transported over a length of optical fiber. At the end of the fiber link, a photodetector (PD) down-converts the RF signals back to the electrical domain. The low loss of the optical fiber allows for the transport of a wide spectrum of signals over lengths from tens to a hundred kilometers. However, the up- and down-conversion that occurs at the beginning and end of the link will degrade the fidelity of the RF signals. To quantify the performance of the link, the key metrics have to be defined.

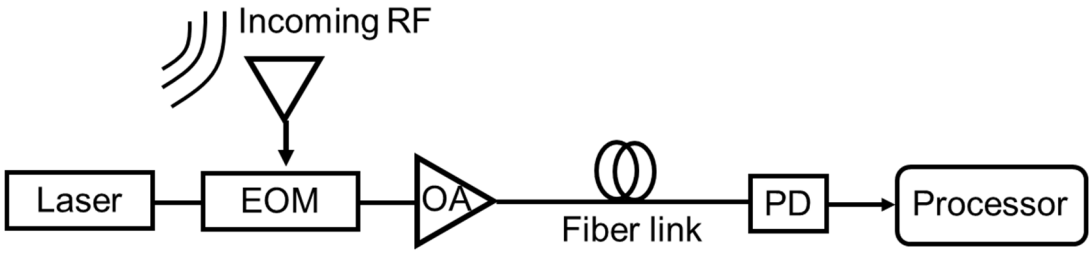

Figure 2. Example of an RF photonic link. EOM: Electro-Optic Modulator, OA: Optical Amplifier, PD: Photodetector

2.1 Metrics for RF Photonic Link

The key performance metrics for an RF photonic link are the RF gain, RF noise figure, the Spur Free Dynamic Range and the Compression Dynamic Range. A graphical representation of the response of the photonic link is shown in Figure 3. From Figure 3, the various metrics can be visualized. The RF gain is the ratio between the output RF power relative to the input RF power. In the log scale, the RF gain (G_{rf}) is the difference between the output RF power and the input RF power, as seen in Equation 1.

$$G_{rf}(dB) = P_{rf,out}(dB) - P_{rf,in}\,(dB) \tag{1}$$

In the example of Figure 3, the output RF power is equal to the input RF power, yielding an RF gain of 0 dB, also referred to as unity gain. If the gain of the link were to change, the fundamental response line will shift up or down on the plot.

The RF Noise Figure, in the log scale, is the difference between the signal to noise ratio at the input of the link and the signal to measured noise ratio at the output of the link. Note that the noise at the input of the link must be at the thermal limit to meet the definition of noise figure. The mathematical definition of RF Noise Figure is presented in Equation 2, where N_{out} is the measure output noise level and the constant of -174 dBm is from Boltzmann's constant multiplied by room temperature of 290 degrees Kelvin. In the example given here, the RF gain is unity and so the RF noise figure can be determined by simply looking at the measured output noise and adding 174 dBm to it. If the gain is not unity than the RF noise figure will increase or decrease by that amount.

$$NF_{rf}(dB) = N_{out}(dBm/Hz) - G_{rf}\,(dB) + 174\ dBm \tag{2}$$

The RF Spur Free Dynamic Range (SFDR) is a measure of the RF input powers over which the output power of the signal is above the output noise while no spurious signals are detected above the output noise. The spurious signals are a result of nonlinear performance in the constituent components of the photonic link. The nonlinear mixing leads to both harmonic spurious signals as well as intermodulation spurious signals. When two RF signals are input to the photonic link, the strongest even order spurs will occur at the second harmonic frequencies as well as the sum and difference of the two input signal frequencies. The strongest odd order spurs appear at the third harmonic frequencies along with the difference of double one signal's frequency minus the other signal's frequency. One advantage of an RF photonic link is the even order nonlinearities can be suppressed, making the odd order spurs the limiting nonlinearity, meaning the SFDR is third-order limited.

The SFDR can be calculated using the Output Intercept Point (OIP). The OIP is measured by plotting the fundamental frequency output power of the system as a function of the input power. In addition, the spurious signals of interest are also plotted. The fundamental response has a slope of one, while the second and third order spurious signal response have a slope of two and three, respectively. The OIP is the output power where the fundamental response line crosses the spurious signal response. For the RF photonic link, the third order nonlinearity (OIP_3) is the dominant one. Knowing the OIP_3, the third-order SFDR is calculated using the output noise as seen in Equation 3.

$$SFDR_3\left(dB \cdot Hz^{2/3}\right) = \frac{2}{3}[OIP_3(dBm) - N_{out}(dBm)] \tag{3}$$

The RF Compression Dynamic Range (CDR) is the range of input fundamental powers over which the output signal is above the noise floor of the system and the output follows the slope of one. The signal power is above the noise floor and follows the ideal response until it begins to roll off. When the measured output power is 1 dB below the ideal response, this input power is referred to as the 1 dB compression point. The compression dynamic range is then calculated using Equation 4. In most RF photonic systems, the compression dynamic range is often much larger than the spurious free dynamic range, due to the nonlinear response of the up and down conversion process that occurs in these systems [4].

$$CDR(dB \cdot Hz) = P_{1dB}(dBm) + 1 - N_{out}(dBm) \quad (4)$$

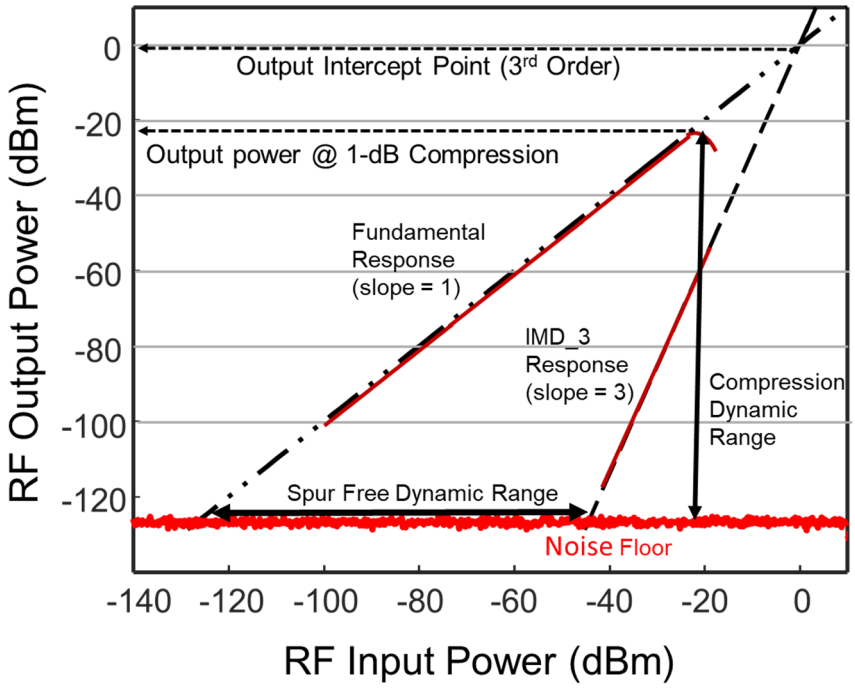

Figure 3. RF metrics represented by a plot of RF input power vs output power

2.2 Architectures of RF Photonic Link

Many different architectures exist for the realization of an RF photonic link. The two main choices involve either direct or external modulation. In direct modulation, the RF signal is modulated onto the optical carrier through the laser drive current. An advantage of direct modulation is the removal of the external modulator, which simplifies the architecture as well as removes a source of optical loss. Unfortunately, direct modulation has disadvantages. The RF gain will always be negative in the dB scale if the slope efficiency is less than one, along with having a limited frequency response and adding frequency chirp to the optical carrier [5].

In terms of externally modulated RF links, phase and intensity modulation are the two primary choices. Phase modulated links use phase modulators to encode the signal onto the phase of the optical carrier, keeping the intensity of the light constant. Advantages of phase modulation include removing the need for a DC bias at the modulator, lower optical loss and potentially higher RF link gain. However, phase modulated links come with some drawbacks. In order to recover the RF signal, the phase modulation has to be converted to intensity before the photodetector. The phase to intensity conversion usually places a limit on the bandwidth of the link [6]. Additionally any phase noise in the laser will be converted to intensity noise, adversely affecting the noise figure and SFDR of the link.

With the various disadvantages of other modulation formats, the most commonly used external modulation uses a Mach Zehnder interferometer based modulator (MZM). The preferred MZM is based on lithium niobate ($LiNbO_3$). Lithium niobate MZMs require no external temperature control and can handle well over 100 milliwatts of optical power. The optical insertion loss is as little as 3 dB and the input RF power can be as high as a watt before failure. In addition, the MZM can be biased to null the even order nonlinear spurs.

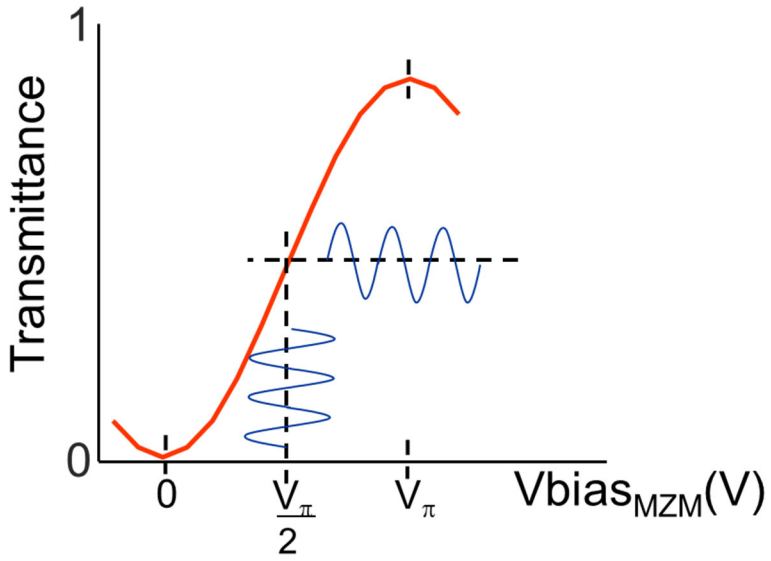

Figure 4 Transfer function of the MZM

2.3 RF Metrics based on Photonic Component Performance

The sinusoidal transfer function of the MZM is shown in Figure 4. When the DC bias point that provides a phase shift of $\pi/2$ is chosen ($V_\pi/2$), the even order terms of the nonlinear transfer function become zero. This operating bias point is often referred to as the Quadrature Bias point. When the MZM is operated at Quadrature, the previous RF metrics can be written in terms of two photonic metrics: the RF V_π of the MZM and the DC photocurrent from the photodetector. Below are the equations to predict the RF performance of the link given these two photonic metrics [6].

$$G_{rf}(dB) = -22.1 + 20\log_{10}\left[\frac{I_{dc}\,(mA)}{V_\pi\,(V)}\right] \tag{5a}$$

$$NF_{rf,shot}(dB) = 22 + 20\log_{10}[V_\pi\,(V)] - 10\log_{10}[I_{dc}\,(mA)] \tag{5b}$$

$$SFDR_{3,shot}\left(dB \cdot Hz^{2/3}\right) = 107.3 + \frac{20}{3}\log_{10}[I_{dc}\,(mA)] \tag{5c}$$

$$CDR_{shot}(dB \cdot Hz) = 151.5 + 10\log_{10}[I_{dc}\,(mA)] \tag{5d}$$

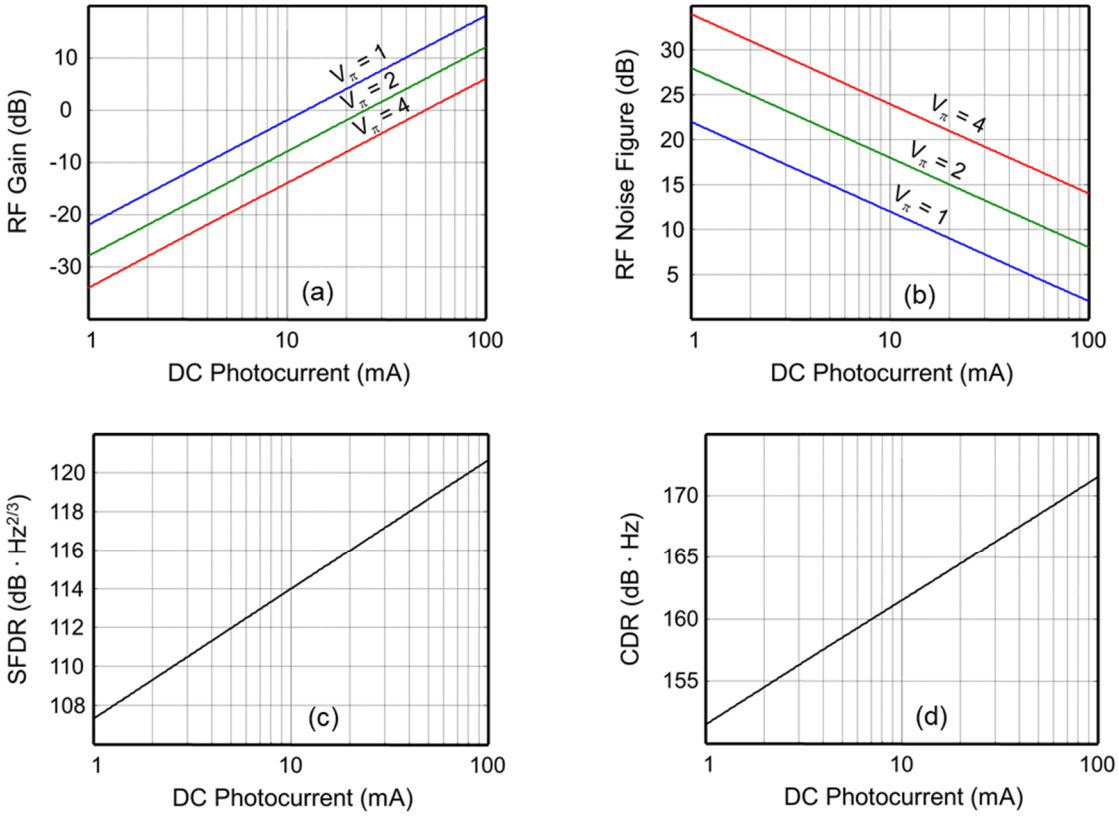

Figure 5 (a) RF gain (b) RF Noise Figure (c) SFDR and (d) CDR as a function of DC photocurrent

Note the equations above assume the input and output of the link are terminated with 50 Ohms and the dominant noise source is shot noise in the link. As an example, the RF gain, Noise Figure, SFDR and CDR as a function of DC photocurrent for a given V_π are plotted in Figures 5 (a-d). Clearly, the higher the DC photocurrent, the higher the RF gain, SFDR and CDR, while the Noise Figure is reduced.

2.4 Advanced RF Photonic Link Architecture

While the V_π of the MZM is fixed, one method for improving the RF metrics is to operate at a different DC bias point. For a link with no optical amplifier, quadrature biasing results in the highest RF gain and allows for cancelling the even order spurs after photodetection. However, in a link with an MZM followed by an optical amplifier, quadrature biasing no longer provides the highest RF gain. In fact, the highest RF gain occurs at a bias lower than quadrature.

The increased RF gain for low-biasing the MZM comes from suppressing the optical carrier as it enters the optical amplifier. When the optical carrier is suppressed to be about the same power as the RF generated sidebands, an increase in the modulation depth occurs, which in turn increases the RF gain of the link. The gain improvement is referred to as all-photonic gain, as it does not depend on any electronic amplification to achieve higher RF output power.

Low-biasing the MZM can significantly improve the RF gain when compared to quadrature biasing the MZM at the same photocurrent [7]. In Figure 6, the quadrature biased link has a gain of around unity, while the low biased link increases the RF gain to about 20 dB. While the output noise increases when low-biased, the gain increase is much more significant. Thus, the noise figure of the link decreases from 33 dB to 21 dB, an improvement of 12 dB.

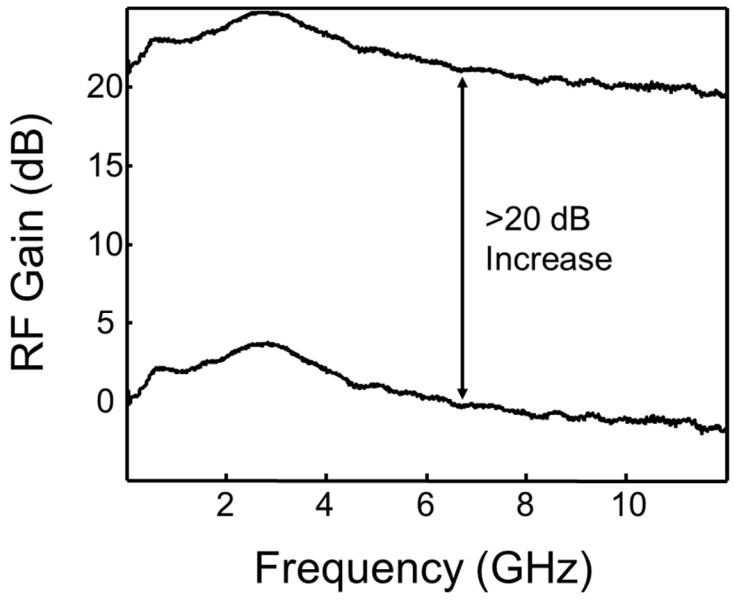

Figure 6. RF gain of a photonic link at quadrature bias and low bias

2.5 RF Photonic Link Summary

The RF photonic link is one of the most used applications of RF photonics. Due its numerous advantages, the external MZM combined with direct detection at a photodetector is the preferred option. Having determined the type of photonic link that will be used, the RF metrics as a function of the photonic component performance can be defined. Finally, the different photonic components metrics are described in relation to the RF metrics.

3.0 Optoelectronic Oscillator Applications

Extremely precise timing is needed for many systems, from radars to sampling clocks. RF photonics can be used to meet these needs by using an architecture known as an optoelectronic oscillator (OEO). The OEO has previously been demonstrated to not only provide low phase noise signals for timing, but also to provide clock recovery. In this section, the OEO architecture will be explored along with different uses for the OEO.

3.1 OEO Architecture

OEOs were first introduced by Yao and Maleki [8] in 1996. As seen in Figure 7, the OEO uses a laser which feeds an electro-optic modulator. The output of the modulator passes along a long optical fiber delay line and into a photodetector. The electrical signal is amplified and sent through an electronic bandpass filter. The filter's output is connected to the RF input of electro-optic modulator, thus completing the optoelectronic cavity. The OEO oscillates when the gain in the optoelectronic cavity exceeds the loss. The frequency of oscillation is determined by the electronic bandpass filter.

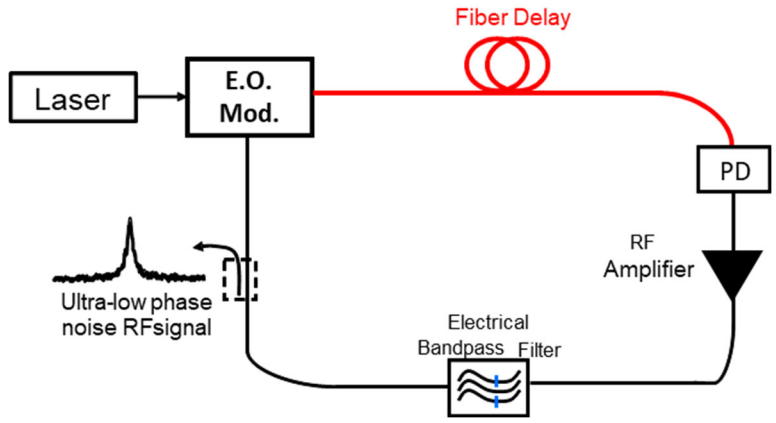

Figure 7: Diagram of a basic optoelectronic oscillator. PD: photodiode, E. O. Mod: Electro-optic modulator

The OEO benefits from the use of ultra-low loss optical fiber in the delay line, resulting in an extremely high Q factor. For an oscillator, the Q factor is the ratio of the stored energy in the cavity over the loss of the cavity. Since the loss of the fiber delay line is ~0.2 dB/km, a long length of fiber can store a large amount of energy with very little loss, achieving Q factors on the order of 10^8 or higher. Such a high Q factor corresponds to a 10 GHz clock signal with a phase noise of -140 dBc/Hz at 10 kHz offset [8]. Note a limit exists in the improvement of the phase noise as the length of fiber increases. Previous work [9] has shown the improvement in the timing jitter, derived from the phase noise, of an OEO has an inverse square root dependence on the fiber length. The limitations are due to the random fiber length variations due to small fluctuations in the environment around the fiber span.

3.2 Metrics of an OEO

Before going into applications for the OEO, the metrics that are important to the performance of an OEO should be discussed. The first metric is the phase noise of the oscillator. When characterizing oscillators of any type, the measurement of the frequency fluctuations is called the phase noise measurement. For the OEO, the commonly accepted definition of the phase noise is the single-side band power spectral density (PSD) of the generated RF signal from the OEO. Denoted in the mathematical expressions as $\mathcal{L}(f)$, the PSD is normalized to the power of the RF signal, thus having the units of dBc/Hz. An example of a measured phase noise PSD of an OEO appears in Figure 7. The phase noise decreases until it reaches a noise floor, which is set by the various components of the OEO, as well as the mode spacing of the cavity.

The second metric is the timing jitter. For most applications, timing jitter is the preferred metric for determining the quality of the clock signal. From the measured phase noise spectrum such as the one in Fig. 8, the total noise can be derived. In general this is written as

$$\sigma_n = \sqrt{2\int_{f_{min}}^{f_{max}} \mathcal{L}(f)df} \tag{6}$$

where σ_n is the total rms noise and f_{max} and f_{min} are the maximum and minimum frequency offsets that the phase noise is integrated over. If the amplitude noise of the signal is negligible, the rms timing jitter (σ_j) can be obtained by the following relationship $\sigma_j = \sigma_n/(2\pi f_{rf})$ with f_{rf} is the RF frequency of the clock. For the example in Figure 8, the calculated timing jitter is 616 fsec.

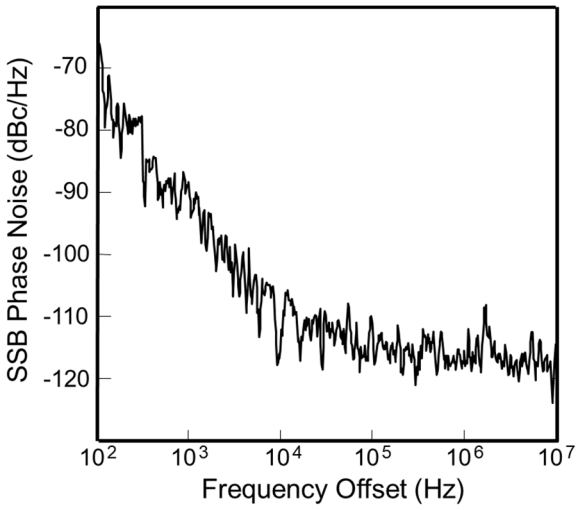

Figure 8: Single side band Phase Noise from an OEO

3.3 OEO for Clock Recovery and Synchronization

Another application of an OEO is for clock recovery and synchronization. The ability to lock two oscillators so that their outputs are synchronized is useful for clock distribution as well as to recover the clock rate of a digital data sequence. The clock recovery process in an OEO is primarily done by the injection locking process. A free-running oscillator's signal can be injected into the OEO. If the frequency of the free-running oscillator is within the locking range of the OEO, the OEO will become locked to the fluctuations of the injected oscillator.

As seen in the following equation, the locking range depends on two factors: the strength of the injected signal (A_{inj}) relative to the free running oscillator's signal strength (A_{free}) and the Q factor of the injected oscillator, as seen in Equation 7,

$$f_{lock} = \left(\frac{A_{inj}}{A_{free}}\right)\left(\frac{f_{free}}{Q}\right). \tag{7}$$

Changing the locking range is usually accomplished in a couple of different ways. By increasing (decreasing) the Q factor of the injected oscillator, the narrower (wider) the range of frequencies over which the oscillator can be locked to the injected signal. The other way involves increasing the power of the injected signal, which will equivalently widen the locking range.

Once the locking range is set, the injected oscillator will follow the phase noise of the incoming signal. Figure 9 shows the calculated PSD of the phase noise, measured in dBc/Hz, as a function of offset frequency from the carrier for an injection locked OEO. The frequency-offset range is between 100 Hz to 10 MHz. The three plotted phase noise curves are labeled $\mathcal{L}_{inj}(\omega)$, $\mathcal{L}_{free}(\omega)$, and $\mathcal{L}_{OEO}(\omega)$, which are the phase noise of the injected signal, the free-running oscillator's output signal, and the phase noise of the locked oscillator's output signal, respectively.

The phase noise of the free-running oscillator, $\mathcal{L}_{free}(\omega)$ and the injected signal, $\mathcal{L}_{inj}(\omega)$, both have a slope of $1/f^2$, denoting white noise as the dominant noise source. In this example, the free-running oscillator phase noise is 20dB lower than the injected signal. For each of three different locking ranges, the injection locked oscillator's phase noise follows the injected signal within the various locking ranges. Once the frequency offset exceeds the locking range, the phase noise decreases to the level of the free running oscillator phase noise.

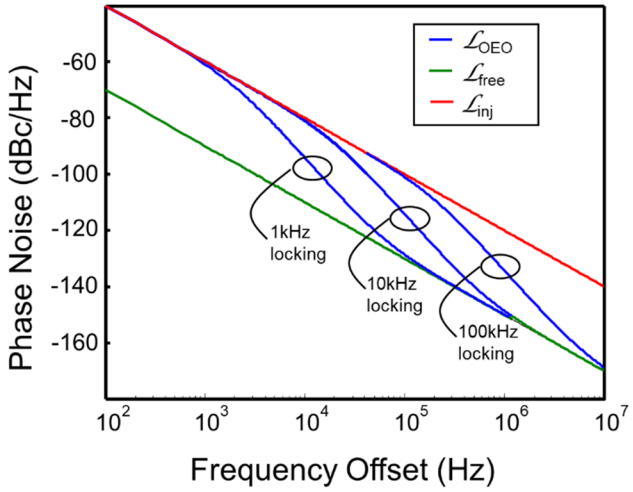

Figure 9: Theoretical plot of the phase noise of an injection locked OEO along with the injected signal and free running OEO's phase noise.

3.4 OEOs with All-Photonic Gain

In order to improve the phase noise of the OEO, components that add noise should be removed. One of the easiest to replace is the electronic amplifier. As seen in the RF link section, the RF gain depends on the V_π of the MZM and the I_{DC} at the photodetector. However, these can be overcome if the MZM is low-biased and followed by an optical amplifier. Since the gain no longer depends on an electronic component, the OEO now utilizes all-photonic gain in order to oscillate. One advantage of the all-photonic gain is it is not limited in its frequency operating range bandwidth as most electronic amplifiers are. The drawbacks in using the all-photonic gain technique is the increase in the second harmonic spurs. In the case of the OEO, the electrical bandpass filter will suppress the second harmonic frequency, making it negligible. In a previous demonstration [11], the all-photonic gain OEO was able to provide up to 13 dB of gain, compensating for the cavity loss and allowing the OEO to oscillate. In addition, the all-photonic gain OEO improved the phase noise when compared to the same OEO using an electrical RF amplifier. In Figure 10,

the phase noise spectrum in the 100 Hz to 1 kHz frequency offset range is dominated by the flicker phase noise of the RF amplifier, which is why the phase noise drops as $1/f^3$. When using the all-photonic gain, the noise is now dominated by white noise in the same frequency offset range, with a decrease of $1/f^2$. Thus, the overall phase noise of the OEO is reduced.

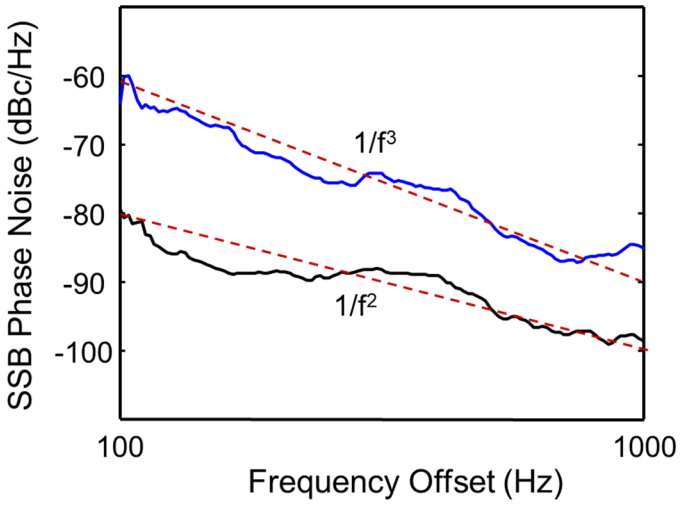

Figure 10: Phase noise of an OEO using all-photonic gain and electronic gain.

3.5 Summary of OEO Applications

The OEO is one of the most versatile demonstrations of RF photonics. It can be used to generate low phase noise signals as well as for clock recover and synchronization. Other applications using OEO include data format conversion [12], RF signal discrimination [13], sensors [14] and broadband chaos generation [15]. The OEO performance can also be improved by utilizing all-photonic gain. By removing the electronic amplifier in the feedback loop, the overall phase noise performance of the oscillator output can be improved. Clearly, the OEO can be used to address many applications.

4.0 Signal Isolation Utilizing RF Photonics

Another application where RF photonics can be used is signal isolation. Many systems required the ability to both transmit and receive signals. As new users continue to make use of the available RF spectrum, new technologies are pushing into higher frequencies in order to meet growing demand. 5G wireless communications has defined a millimeter wave band in the 30 GHz range for high bandwidth, short reach networking. Accessing higher frequencies is one of the key motivations for using RF photonics. In this section, signal isolation utilizing RF photonics will be discussed.

4.1 Methods for Signal Isolation

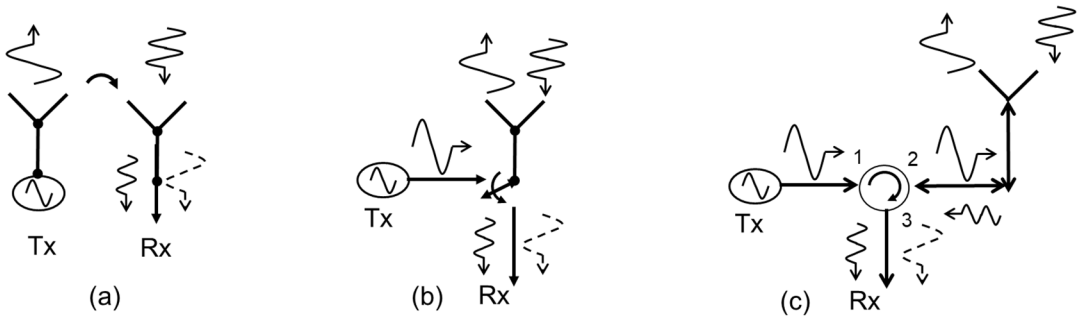

Figure 11: (a) Two independent antennas for signal isolation. (b) A single antenna followed by a transmit/receive switch. (c) An RF circulator connected to a single antenna for transmit and receive isolation.

One method for signal isolation is to make the transmit signal's frequency different than the receive signal's frequency. Then, isolation is simply accomplished by using the appropriate set of filters to remove the unwanted signal. The larger the separation between the frequencies, the higher the isolation can be. However, some applications will require the transmit and receive signals to be the same frequency. A method to accomplish this is to use two separate antennas, where one is used solely for receive while the other only transmits. Isolation between the receive and transmit signals is then achieved simply by physically spacing the two antennas apart from each other, even though some transmit signal will couple into the receive antenna, as seen in Figure 11(a). On the other hand, using a single antenna for both transmission and reception would reduce the required space. Given this limitation, isolation can be accomplished in a couple of different ways. The first method for isolation using a single antenna is to use time gaiting [16]. By using a high speed switch, the system can transmit a signal for a set period of time, and then switch to the receive path, as seen in Figure 11(b). While this addresses the need for a single frequency to be both transmitted and received, it does not allow for concurrent transmission and reception. To address continuous transmit and receive, an RF circulator is used right after the antenna, as appears in Figure 11(c). The circulator is a three port component, with the transmit signal entering port 1 and passed onto port 2 with very low loss. Port 2 is connected to the antenna, where signals can be transmitted and received simultaneously. The received signal enters port 2 and passed to port 3 with low loss. The losses between ports 1 and 3 are very high, as well as the loss for any signal entering port 2 and leaking out to port 1. Thus, the RF circulator provides low loss paths between the transmit and receive paths and high isolation between the two paths. Current RF circulator technology is limited to narrow frequency bandwidths while still providing high isolation. Demonstrations have shown isolation of 40 dB on a 2.4 GHz signal with 100 MHz of signal bandwidth [17]. Other demonstrations have shown 10 dB of isolation at frequencies up to 20 GHz [18]. At higher frequencies, the isolation begins to degrade while the insertion loss increases.

4.2 RF Photonic Architecture for Signal Isolation

An RF photonic solution can provide large isolation of the transmit and receive paths from a single antenna over a wide frequency range. One configuration that combines multiplexing single side band modulation with a bi-directional signal interface using an optical modulator appears in Figure 12 [19]. The photonic technique can be seen as a three port RF circulator. The transmit signal connects to port 1 and is then split by a 90 degree hybrid onto the two RF waveguide electrodes in an MZM. The top electrode is connected to the 0 degree output of the hybrid, while the bottom electrode is connected to the 90 degree output. The

signals are recombined at a second hybrid whose inputs are complementary to the first hybrid. In the given example, the top electrode connects to the 90 degree input of the second hybrid, while the bottom electrode connects to the 0 degree input. The combined transmit signal exits through port 2 and out to the antenna. Simultaneously, any receive signal from the antenna enters port 2 and is split onto the RF electrodes by the 90 degree hybrid. The receive signal is then modulated onto the laser carrier. Finally, the modulator's optical output connects to a photodetector, which recovers the RF signal back into the electrical domain. This output is port 3 of an equivalent three port circulator.

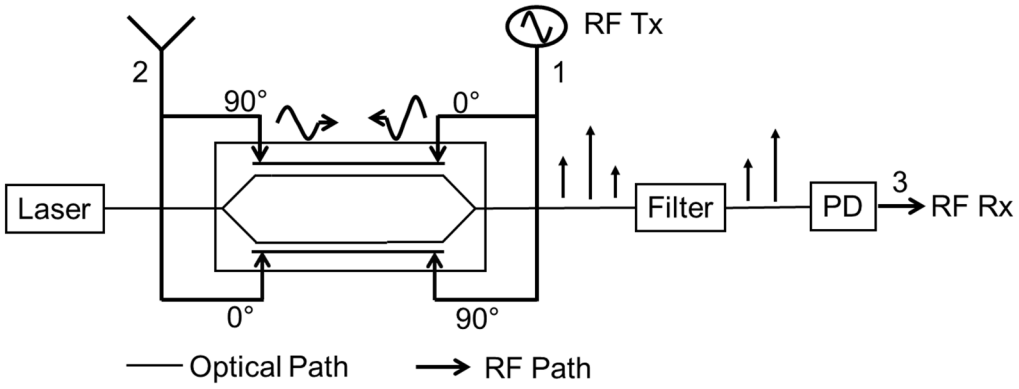

Figure 12: An RF photonic based circulator for isolating transmit and receive paths.

In Figure 12, the transmit signal moves from right to left, while the receive signal moves from left to right. The optical field from the laser that enters the MZM also moves from left to right. Ideally, the receive signal, which co-propagates with the optical field in the MZM, will be optimally modulated onto the laser carrier, while the transmit signal, which counter-propagates with respect to the optical field in the MZM, will not be modulated at all onto the laser carrier. However, previous work [20] has shown the transmit signal will still be modulated onto the optical carrier, though much less efficiently.

The use of a 90 degree hybrid allows for single side band modulation [21], which can address the leakage of the transmit signal onto the optical carrier. The optical sideband that contains the RF signal depends on the orientation of the 90 degree hybrid. In this example, the receive signal will appear on the upper optical sideband of the carrier. For the transmit signal, the 90 degree hybrid is placed in a complementary configuration, resulting in its appearance on the lower optical sideband of the carrier. Even though the transmit and receive signals are the same frequency, they are now separated on either side of the optical carrier. In order to isolate the receive signal from the transmit signal at port 3, an optical filter can be used to remove the unwanted optical side band before photodetection. The recovered RF signal is then just the receive signal.

The RF photonic-based circulator can provide many advantages. By filtering the transmit signal, the isolation between port 1 and port 3 can be theoretically infinite, while the losses between port 1 and port 2 are relatively low. The configuration can potentially provide improvements even when reflections from the antenna are taken into account. In terms of drawbacks, the connection between port 2 and port 3 is an active link, so issues such as RF loss, linearity and noise figure become significant. Similar metrics for a single

side band link have already been developed [21] and can be applied to this configuration to estimate the RF performance. Any application will have to account for these metrics before using this solution.

4.3 Further Applications of RF Photonics to Signal Isolation

RF photonics can be used to address the needs of signal isolation and separation. As the RF spectrum becomes more congested, the ability to pull specific signals will continue to be a needed function. The photonic based RF circulator can address some RF isolation needs. Other RF photonic filtering techniques, including optical bandpass and notch filters [22] as well as photonic based Finite Impulse Response (FIR) filters [23] can address RF separation needs. The optical filter techniques provide benefits of very narrow passbands at very high center frequencies. These types of filters can also be tuned [24], allowing them to adapt to a changing RF environment.

5.0 Conclusions

RF photonics can be applied to address multiple needs. While three specific examples have been provided, several other applications exist. For example, an analog link can also be used for analog delay lines, or analog memory units. Multiple demonstrations have been made of analog delay lines that cover very wide frequency ranges with low noise and high RF gain [25]. Photonics can also play a role in systems that seek to minimize interference in congested RF environments [26].

Another application utilizing RF photonics is for signal identification. Wideband RF spectrum analyzers can be developed based on photonic components [27]. Channelization can also be accomplished using optical filters. These filters can be used to reduce a wideband RF spectrum into multiple smaller bandwidth channels, allowing for more efficient processing of the overall spectrum. [28]. Downconversion of high frequency signals can also be addressed with RF photonics, with demonstrations including frequency combs [29] and other architectures [7].

While most of these demonstrations have been made using discrete components, future applications will use integrated photonic circuits. Advantages provided by integrated photonic circuits include size and weight reductions, while also driving down the costs of RF photonic systems. Foundry access allows for the design and fabrication of photonic circuits in both silicon and III-V semiconductor materials [30].

The possible applications for RF photonics continues to expand in ways that cannot be absolutely predicted. With the continued need to access higher frequencies, RF photonics is well suited to address these needs. The future will continue to see an expansion of the use of RF photonics long with improvements to performance and reliability.

References

1. M. Shafi, A. F. Molisch, P. J. Smith, T. Haustein, P. Zhu, P. De Silva, F. Tufvesson, A. Benjebbour, and G. Wunder. "5G: A Tutorial Overview of Standards, Trials, Challenges, Deployment, and Practice." IEEE Journal on Selected Areas in Communications, Vol. 35, No. 6, pp. 1201-1221, Jun. 2017.
2. T. Berceli and P. Herczfeld, “Microwave Photonics – A Historical Perspective”, IEEE Microwave Theory and Techniques, Vol. 58, No. 11, pp. 2992-3000, Nov 2010.

3. J. Dreher, Phase Stability of ATA Fiber Optic Cables, Seti Institute, ATA Memo 55, March 2003.
4. V. Urick, F. Bucholtz, J. McKinney, P. Devgan, A. Campillo, J. Dexter and K. Williams, “Long Haul Analog Photonics,” IEEE Journal of Lightwave Technology, Vol. 29, No. 8, pp. 1182-1205, 2011.
5. C. Cox, E. Ackerman, G. Betts and J. Prince, “Limits on the Performance of RF-over-Fiber Links and Their Impact on Device Design,” IEEE Transactions on Microwave Theory and Techniques, Vol. 54, No. 2, pp. 906-920, 2006.
6. V. J. Urick, J. D. McKinney and K. J. Williams, Fundamentals of Microwave Photonics, John Wiley & Sons, 2015.
7. P. Devgan, Applications of Modern RF Photonics, Artech House, 2018.
8. X. S. Yao and L. Maleki, "Optoelectronic Oscillator for Photonic Systems," IEEE Journal of Quantum Electronics, Vol. 32, No. 7, pp. 1141-1149, 1996.
9. J. Lasri, P. Devgan, R. Tang, and P. Kumar, “Self-starting Optoelectronic Oscillator for Generating Ultra-Low-Jitter High-Rate (10GHz or higher) Optical Pulses,” Optics Express, Vol. 11**,** No. 12, pp. 1430-1435, 2003.
10. P. Devgan, D. Serkland, G. Keeler, K. Geib, and P. Kumar, “An Optoelectronic Oscillator Using an 850nm VCSEL for Generating Low Jitter Optical Pulses,” IEEE Photonics Technology Letters, Vol. 18, No. 5, pp. 685-687, 2006.
11. P. S. Devgan, V. J. Urick, J. F. Diehl, and K. J. Williams, “Improvement in the Phase Noise of a 10 GHz Optoelectronic Oscillator Using All-Photonic Gain,” IEEE Journal of Lightwave Technology, Vol. 27, No. 15, pp. 3189-3193, 2009.
12. J. Lasri, P. Devgan, V. S. Grigoryan and P. Kumar, “Multiwavelength NRZ-to-RZ Conversion with Significant Timing-Jitter Suppression and SNR Improvement,” Optics Communications, Vol. 240, No. 4–6, pp. 293-298, 2004.
13. P. S. Devgan, V. J. Urick and K. J. Williams, “Detection of Low-Power RF Signals Using a Two Laser Multimode Optoelectronic Oscillator,” IEEE Photonics Technology Letters, Vol. 24, No. 10, pp. 857-859, 2012.
14. N. Duy, B. Journet, I. Ledoux-Rak, J. Zyss, L. Nam and V. Luc, "Opto-Electronic Oscillator: Applications to Sensors," Proceedings of IEEE Microwave Photonics Meeting, pp. 131-134, 2008.
15. K. Callan, L. Illing, Z. Gao, D. Gauthier, and E. Schöll, “Broadband Chaos Generated by an Optoelectronic Oscillator,” Physics Review Letters, Vol. 104, No. 11, pp. 113901-113904, 2010.
16. M. Skolnik, Radar Handbook, McGraw-Hill Education, 2008.
17. T. Huusari, Y. Choi, P. Liikkanen, D. Korpi, S. Talwar and M. Valkama, "Wideband Self-Adaptive RF Cancellation Circuit for Full-Duplex Radio: Operating Principle and Measurements," IEEE 81st Vehicular Technology Conference*,* pp. 1-7, 2015.
18. E. F. Schloemann, "Circulators for Microwave and Millimeter-Wave Integrated Circuits," Proceedings of the IEEE*,* Vol. 76, No. 2, pp. 188-200, 1988.
19. E. Ackerman, C. Cox, H. Roussell and P. Devgan, “Broadband Simultaneous Transmit and Receive from a Single Antenna Using Improved Photonic Architecture,” IEEE International Microwave Symposium, 2019.
20. G. K. Gopalakrishnan, W. K. Burns, R. W. McElhanon, C. H. Bulmer and A. S. Greenblatt, "Performance and Modeling of Broadband $LiNbO_3$ Traveling Wave Optical Intensity Modulators," IEEE Journal of Lightwave Technology, Vol. 12, No. 10, pp. 1807-1819, 1994.
21. P. Devgan, D. Brown, and R. Nelson, "RF Performance of Single Sideband Modulation Versus Dual Sideband Modulation in a Photonic Link," IEEE Journal of Lightwave Technology, Vol. 33, No. 9, pp.1888-1895, 2015.

22. J. Capmany, B. Ortega, and D. Pastor, "A Tutorial on Microwave Photonic Filters," IEEE Journal of Lightwave Technology, Vol. 24, No. 1, pp. 201-229, 2006.
23. J. Zhao, H. Zhang, Z. Yang, J. Xu, T. Xu, and C. Wang. "Few-Mode Fibers with Uniform Differential Mode Group Delay for Microwave Photonic Signal Processing." IEEE Access, Vol. 8, pp. 135176-135183, 2020.
24. Y. Yan and J. Yao, "A Tunable Photonic Microwave Filter with a Complex Coefficient Using an Optical RF Phase Shifter," IEEE Photonics Technology Letters, Vol. 19, No. 19, pp. 1472–1474, 2007.
25. J. F. Diehl, J. M. Singley, C. E. Sunderman, and V. J. Urick, "Microwave Photonic Delay Line Signal Processing," Applied Optics, Vol. 54, No. 31, pp. F35-F41, 2015.
26. V. J. Urick, M. E. Godinez, and D. C. Mikeska, "Photonic Assisted Radio-Frequency Interference Mitigation," Journal of Lightwave Technology, Vol. 38, No. 6, pp. 1268-1274, 2020.
27. F. Schlottau, M. Colice, K. H. Wagner and R. Babbitt, "Spectral Hole Burning for Wideband, High-Resolution Radio-Frequency Spectrum Analysis," Optics Letters, Vol. 30, No. 22, pp. 3003-3005, 2005
28. D. B. Hunter, L. G. Edvell, and M. A. Englund, "Wideband Microwave Photonic Channelised Receiver," Meeting on Microwave Photonics, 2005.
29. A. Agarwal, J. M. Dailey, P. Toliver, and T. C. Banwell, "Photonically-Enabled RF Front-End for Wideband Flexible Down-Conversion," Optics Express, Vol. 25, No. 7, pp. 7338-7348, 2017.
30. http://www.aimphotonics.com